

# Redistribution and Relaxation of Vibrational Excitation of CH-Stretching Modes in 1,1-Dichloroethylene and 1,1,1-Trichloroethane

I. Hartl and W. Zinth\*

Ludwig-Maximilians-Universität München, Institut für Medizinische Optik, Oettingenstrasse 67, 80538 Munich, Germany

Received: August 25, 1999; In Final Form: November 10, 1999

Anti-Stokes Raman scattering after resonant infrared excitation with femtosecond light pulses was used to monitor the vibrational excitation of the CH-stretching modes of liquid  $\text{CH}_2\text{CCl}_2$  and  $\text{CH}_3\text{CCl}_3$ . Selective excitation and probing allowed determination of the various time-constants for the redistribution between the CH-stretching modes and their relaxation. For the symmetric CH-stretching mode of  $\text{CH}_2\text{CCl}_2$  relaxation times of 3.5 and 9.5 ps are determined for the transfer to overtones and to the asymmetric CH-stretching mode, respectively. For  $\text{CH}_3\text{CCl}_3$  these time constants are 5.0 and 4.7 ps.

## 1. Introduction

Ultrafast photochemical reactions on the time scale of 100 fs have been found to be connected with pronounced wave-packet-like modulation of optical signals, indicating the presence of strong vibrational excitation.<sup>1,2</sup> At present there is no detailed understanding of the interconnection between chemical reactions and specific nuclear motions.<sup>3–5</sup> In this context a better knowledge of vibrational excitation, exchange of vibrational energy between specific vibrational modes, and its relaxation out of the molecule is of major interest. In the condensed phase at room temperature the time scale of these processes was found to be on the order of  $10^{-12}$  s.<sup>6–10</sup> However, even with the present possibilities of ultrafast technologies, the fast relaxation, the small cross sections, and the related small signal amplitudes impose considerable difficulties for direct observation of the vibrational population. As a consequence most experiments performed in the past had limited sensitivity and spectral or temporal resolution, thus not allowing a direct and complete analysis of fast transfer reactions between “similar” molecular modes.<sup>11</sup>

Recently we presented an experimental system which allows the observation of vibrational population with subpicosecond temporal resolution.<sup>12</sup> In the present paper we will use this setup to study the relaxation of vibrational energy between and out of CH-stretching modes. Of special importance is the possibility of using selective excitation and specific frequency resolved observation of the symmetric and asymmetric CH-stretching modes. Combined with the high temporal resolution of the experiment this feature allows one to follow independently the population changes of the two vibrational modes. This type of experiment yields the complete set of rate constants for energy transfer between and out of the CH-stretching modes which can be compared with simple theoretical approaches.

## 2. Materials and Methods

The sample molecules 1,1-dichloroethylene and 1,1,1-trichloroethane were obtained from Merck No. 803209 (1,1-dichloroethylene) and No. 108749 (1,1,1-trichloroethane) at purities

of >99% and >99.5%, respectively. The sample was dissolved in  $\text{CCl}_4$  (Merck No. 102209) at concentrations of 1:1 (1,1-dichloroethylene) and 1:2 (1,1,1-trichloroethane) v/v. In the time-resolved measurements the sample volume was exchanged between two subsequent excitation processes in order to prevent heating of the sample.

Stationary characterization was performed as follows: The spontaneous Raman spectra were recorded with a similar experimental setup as used in the transient experiment (see below) with some modifications: 5 mW of the 488-nm line of an  $\text{Ar}^+$  laser was used as laser source and the spectrometer was equipped with a 1800 groves/mm grating to achieve a higher spectral resolution ( $<1.5 \text{ cm}^{-1}$ ). The Raman scattered light was detected in the backward direction ( $180^\circ$  excitation-detection geometry). The solid lines in Figures 1a and 2a show the spectrum recorded with parallel polarization of laser and detection; the broken curve was recorded with crossed polarization. The infrared spectra were measured with a Bruker IFS-66 FTIR spectrometer set to a spectral resolution of  $4 \text{ cm}^{-1}$ .

The experimental system for the time-resolved experiments has been previously described in detail.<sup>12</sup> Here only the important features for the present experiment are given: Vibrational relaxation is measured in an excite-and-probe experiment with subpicosecond light pulses. Tunable infrared pulses are used to excite specific vibrational modes while anti-Stokes Raman scattering of a delayed probing pulse at 815 nm monitors the vibrational excitation.<sup>11</sup> The experiment was operated at a repetition rate of 1000 Hz. The IR pulses had a spectral width of  $100 \text{ cm}^{-1}$ , a duration of 120 fs, and an energy of  $\approx 2 \mu\text{J}$ . They were focused at a beam diameter of  $100 \mu\text{m}$ . The probing “laser” pulses were adjusted to have a spectral width of  $45 \text{ cm}^{-1}$ . By this method a width of the instrumental response function of 700 fs was obtained which was determined by the duration of spectrally narrow probing pulses. To reduce artifacts due to rotational depolarization, pump and probe pulses had a relative polarization of  $65^\circ$ .<sup>13–15</sup> In the experiments the anti-Stokes signal was recorded over three runs of the delay line with an averaging time for each setting of the delay line of 120 s. The signal background, recorded before excitation, i.e., at delay times  $\approx -2$  ps, was subtracted. The disturbing signal spikes by sphaerics (cosmic rays hitting the sensitive area of the CCD detector),

\* Corresponding author. E-mail: zinth@physik.uni-muenchen.de. Fax: +49 89 21782902.

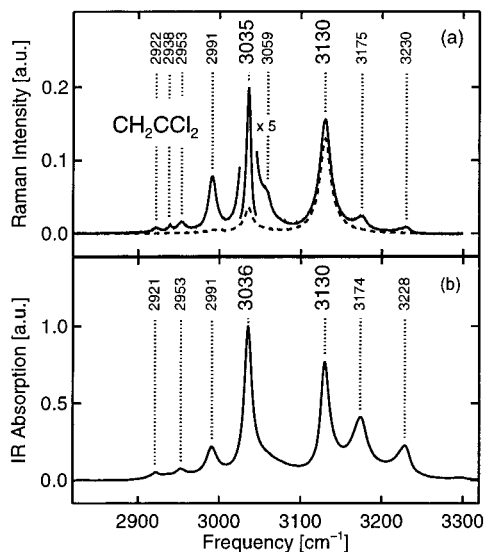


**Figure 1.** Raman (a) and infrared spectrum (b) of 1,1-dichloroethylene in the region of the CH-stretching modes. The Raman spectrum was recorded with parallel (solid line) and perpendicular (broken line) polarization of laser and detection. It shows fundamentals at 3035  $\text{cm}^{-1}$  ( $\nu_1$ ) and 3130  $\text{cm}^{-1}$  ( $\nu_7$ ). It is interesting to note that all bands besides the anti-symmetric CH-stretching vibration  $\nu_7$  are polarized.

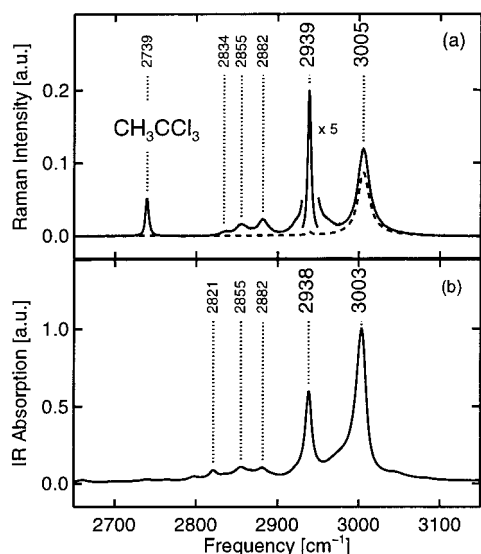


**Figure 2.** Raman (a) and infrared spectrum (b) of 1,1,1-trichloroethane in the region of the CH-stretching modes. The Raman spectrum was recorded with parallel (solid line) and perpendicular (broken line) polarization of laser and detection. It shows the fundamentals at 2939  $\text{cm}^{-1}$  ( $\nu_1$ ) and 3005  $\text{cm}^{-1}$  ( $\nu_7$ ).

visible at large averaging times, were removed. The anti-Stokes energy is a direct measure of the vibrational excitation of the observed mode. To compare the relative population of the two modes one has to scale the signals by their respective Raman cross sections.

The analysis of the experimental data was performed with the rate equation system shown in Figure 6, where the different CH-stretching modes are considered explicitly. Irreversible decay of the population out of these modes ( $\nu_1$  and  $\nu_7$  in our case) is assumed to occur via microscopic rates  $\gamma_{01}$  and  $\gamma_{07}$ . The transfer between these modes was described by the rates  $\gamma_{71}$  and  $\gamma_{17}$ . When a state is degenerate (such as  $\nu_7$  in 1,1,1-trichloroethane) it was treated in the reaction model as a pair of states with fast internal population transfer. Within this model the experimentally detectable population changes are described

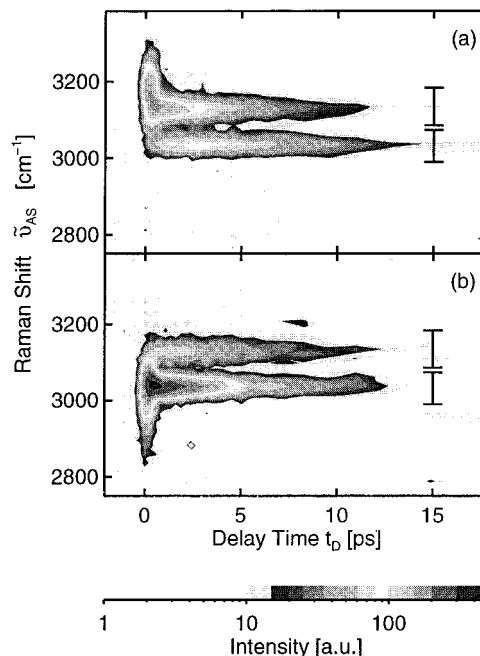


**Figure 3.** Anti-Stokes Raman signal of 1,1-dichloroethylene plotted as function of Raman shift and delay time. At  $t_D = 0$  a short excitation laser pulse centered at 3140  $\text{cm}^{-1}$  (a) and 3020  $\text{cm}^{-1}$  (b) was applied to the sample. At later times the Raman signal of the two CH-stretching modes can clearly be separated. The decay of the individual modes can be clearly observed. The bars indicate the spectral range used when displaying the integrated intensities in Figure 4.

by the sum of exponentials, where the time constants are related to the eigenvalues of the matrix of microscopic rates  $\gamma_{ij}$ . Since different starting populations of  $\nu_1$  and  $\nu_7$  can be achieved by tuning the excitation wavelength, mode selective observation yields enough information (namely, the two eigenvalues  $1/\tau_i$  and the relative populations) to deduce the microscopic rates of the reaction model.

For data handling the experimental points were integrated over the bandwidth of 95  $\text{cm}^{-1}$  (1,1-dichloroethylene) and 70  $\text{cm}^{-1}$  (1,1,1-trichloroethane). The data were fitted by a model function consisting of two exponentials convolved by the instrumental response function. The contribution of a fast decaying signal from overtones, combination bands, or optical nonlinearities is considered via an additional term proportional to the instrumental response function. The initial populations of the CH-stretching modes in the experiments are determined by extrapolating the exponential functions back to  $\tau_D = 0$ .

### 3. Vibrational Spectra

**1,1-Dichloroethylene.**  $\text{CH}_2\text{Cl}_2$  has two CH-stretching modes which are both Raman and IR active. The antisymmetric CH-stretching mode  $\nu_7$  is at 3130  $\text{cm}^{-1}$ , the symmetric  $\nu_1$  mode at 3035  $\text{cm}^{-1}$ . Of special interest for the relaxation of vibrational energy out of the CH-stretching modes are overtone and combination modes anharmonically coupled to the fundamentals.<sup>16</sup> The Raman spectrum, Figure 1a, displays such bands at 2922, 2938, 2953, 2991, 3059, 3175, and 3230  $\text{cm}^{-1}$ . These bands obtain their intensities via Fermi resonance from the symmetric  $\nu_1$  mode. This connection can be deduced from the observation that these bands are strongly polarized (see solid and broken curve in Figure 1a) and thus belong to the  $A_1$  symmetry type. Some of these bands also show up in the IR spectrum of Figure 1b. An assignment of the different bands has been given in refs 17 and 18.

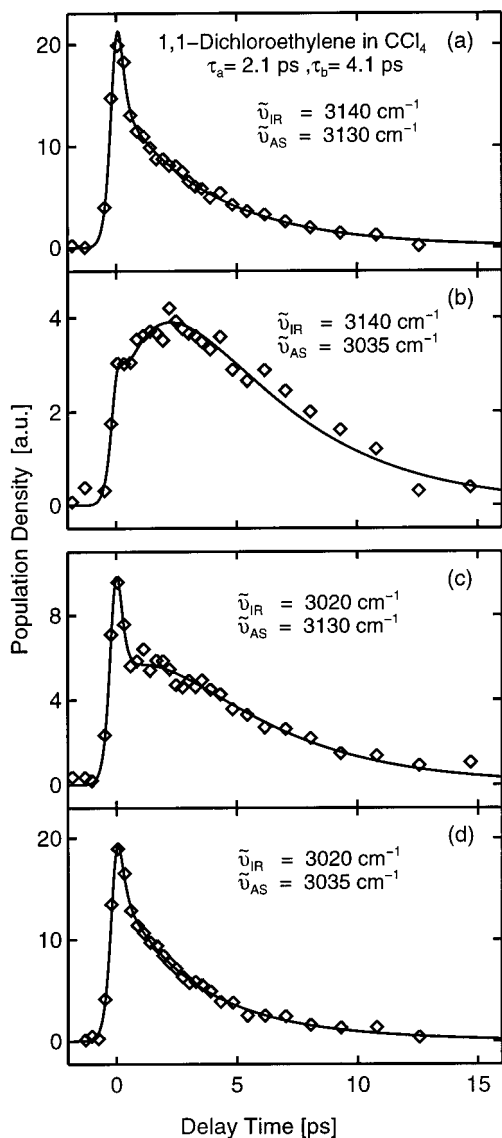


**Figure 4.** Vibrational population after excitation of the antisymmetric (a, b) and the symmetric (c, d) CH-stretching vibration of 1,1-dichloroethylene at time  $t_D = 0$ . The data points (diamonds) are obtained by spectral integration over the Raman bands (see Figure 3) and scaling by their respective Raman cross sections. The solid line shows a biexponential fit with the time constants 2.1 and 4.1 ps. In the model curve a contribution of the instrumental response function was added in order to account for nonlinear processes found at time zero.

**1,1,1-Trichloroethane.** In 1,1,1-trichloroethane (see Figure 2) the two CH-stretching modes are also Raman and IR active. The asymmetric CH-stretching mode  $\nu_7$  at  $3005\text{ cm}^{-1}$  is degenerate. The symmetric CH-stretching mode is found at  $2939\text{ cm}^{-1}$ . Again the Raman and IR spectra display a number of overtone and combination bands in the range between 2700 and  $3350\text{ cm}^{-1}$ . Most important for relaxation out of the CH-stretching modes seem to be the bands at 2739, 2834, 2855, and  $2882\text{ cm}^{-1}$  which are well seen in the Raman spectrum. Due to the polarization of the Raman spectra, one can state that these modes are coupled to the symmetric CH-stretching vibration  $\nu_1$ . Detailed assignments of these modes have been given in the literature.<sup>19,20</sup>

In both samples, the large spectral width of the exciting IR pulses ( $\approx 100\text{ cm}^{-1}$ ) prevents the excitation of a single vibrational transition. To generate starting populations with strong differences in the population of the symmetric and antisymmetric CH-stretching modes, the spectral position of the IR pulses is

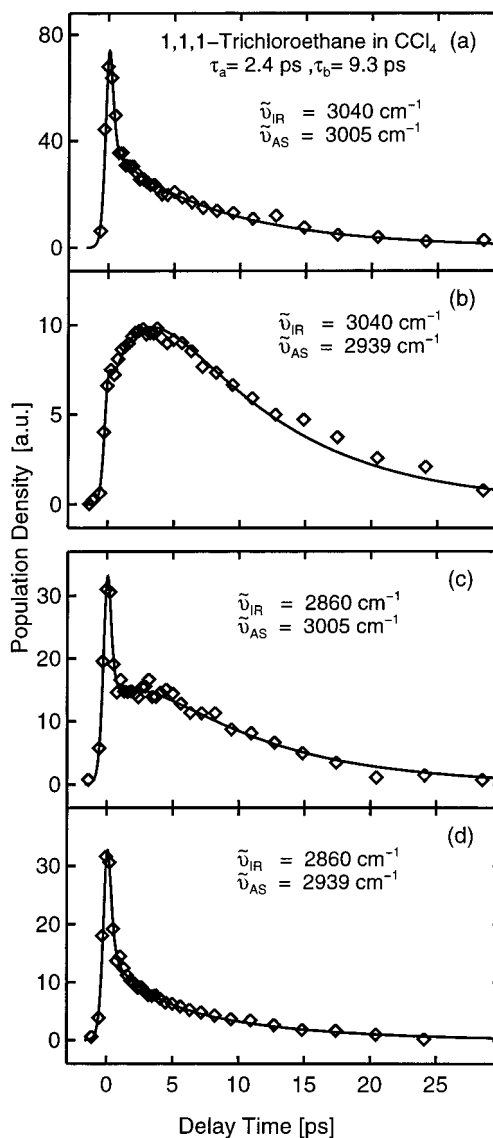


**Figure 5.** Vibrational population after excitation of the degenerate (a, b) and the symmetric (c, d) CH-stretching vibration of 1,1,1-trichloroethane at time  $t_D = 0$ . The data points (diamonds) are obtained by spectral integration over the Raman bands (integration range:  $70\text{ cm}^{-1}$ ) and scaling by their respective Raman cross sections. The solid line shows a biexponential fit with the time constants 2.4 and 9.3 ps. In the model curve a contribution of the instrumental response function was added in order to account for nonlinear processes found at time zero.

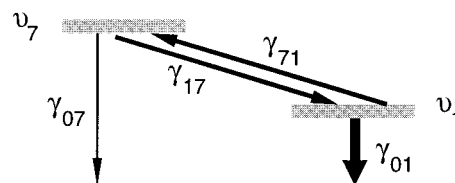


**Figure 6.** Reaction model for the vibrational energy transfer between and out of the CH-stretching modes. The amplitudes and time constants from the biexponential fit of the experimental data and the principle of detailed balance were used to obtain the microscopic reaction rates  $\gamma_{ij}$  presented in Table 1.

shifted to the red or the blue wing of the CH-stretching region. In this way we obtain a predominant population of one of the fundamentals. However, there is always an additional excitation of overtone and combination bands. This can lead to fast initial transients in the Raman signal. In the qualitative analysis of

the experimental data we considered this contribution by fitting it with the instrumental response function (see above).

#### 4. Time-Resolved Observations

**4.1. 1,1-Dichloroethylene.** A gray scale plot of the anti-Stokes Raman signal vs delay time is shown in Figure 3 for the two different excitation wavelengths used. At delay time zero the signal is concentrated around the anti-Stokes frequency related to the spectrum of the exciting IR pulse ( $3140\text{ cm}^{-1}$ , Figure 3a, and  $3020\text{ cm}^{-1}$ , Figure 3b). This interesting feature may be caused by the driving of the vibrations (fundamentals and overtones) with the IR pulse or due to a nonlinear background.<sup>21</sup> At later delay times the individual signals from the two CH-stretching modes can be well followed. For the initially excited mode we see a continuous decay, while for the other mode a delayed rise of the signal can be observed. Figure 4 displays the time-dependence of the anti-Stokes signal for the two bands obtained by integrating over the spectral range indicated by the bars in Figure 3. Figure 4a,b represents results for the high-frequency excitation case: For the initially excited anti-Stokes CH-stretching mode one finds—after the rapid decay of the signal due to the instantaneous sample response—a decrease which extends over more than 10 ps (Figure 4a). For the symmetric CH-stretching mode (Figure 4b) the instantaneous part of the signal is followed by a signal rise before the signal starts to decay after  $t_D = 3$  ps. When the low-frequency excitation in the symmetric CH-stretching mode is used (Figure 4c,d) one observes well the decay of the signal for both modes at later delay times. A delayed rise of the signal is not evident for the accepting high frequency mode where one only observes a plateau at early delay times (Figure 4c). The results from a modeling of these data yield a detailed description of the reaction processes: After the instantaneous response the data points of all four curves are fitted well by biexponential functions with the time constant  $\tau_a = 2.1 \pm 0.3$  ps and  $\tau_b = 4.1$  ps  $\pm$  0.6 ps. The choice of the same two time constants for all four signal traces is a consequence of the reaction model with two vibrational states.

**4.2. 1,1,1-Trichlorethane.** In Figure 5 the observations on  $\text{CH}_3\text{CCl}_3$  are shown for the two IR excitation pulses centered at  $3040\text{ cm}^{-1}$  (Figure 5a,b) and  $2860\text{ cm}^{-1}$  (Figure 5c,d). Qualitatively the anti-Stokes signals of the degenerate asymmetric ( $\nu_{\text{AS}} \approx 3005\text{ cm}^{-1}$ ) and the symmetric CH-stretching mode ( $\nu_{\text{AS}} = 2939\text{ cm}^{-1}$ ) behave in a similar way to the ones observed for 1,1-dichloroethylene. A fast instantaneous response due to driven modes and nonlinear coupling is followed by a biexponential decay for the two situations where excitation and probing is done on the same mode (Figure 5a,d). In the case of an initial excitation transfer to the observed mode (Figure 5b,c), the rise with  $\tau_a$  precedes the slower decay with  $\tau_b$ . In  $\text{CH}_3\text{CCl}_3$  the two time constants are found to be  $\tau_a = 2.4 \pm 0.3$  ps and  $\tau_b = 9.3 \pm 1$  ps.

#### 5. Discussion

Qualitatively the experimental observations can be summarized as follows:

When excitation and probing is on the same mode, one observes a continuous decay of the signal, which is biexponential.

When excitation is at a higher frequency than probing, the population shows first a rise and a subsequent decay.

The population changes can be modeled for both molecules by two time constants.

**TABLE 1: Time Constants for Relaxation and Redistribution**

	time constants, ps			
	relaxation of		redistribution of	
	symmetric mode $1/\gamma_{01}$	asymmetric mode $1/\gamma_{07}$	asymmetric to symmetric mode $1/\gamma_{17}$	symmetric to asymmetric mode $1/\gamma_{71}$
$\text{CH}_2\text{CCl}_2$	3.5	8.6	5.9	9.5
$\text{CH}_3\text{CCl}_3$	5.0	16.2	6.7	4.7

**TABLE 2**

$\omega_j$	$R_j$	$T_{2j}$ , ps	$1/\Gamma_{j1}$ , ps
a			
2922	0.0047	0.74	471.3
2938	0.0047	1.04	599.0
2953	0.019	0.56	74.5
2991	0.11	0.53	10.3
3059	0.079	0.37	8.0
3175	0.051	0.27	20.6
3230	0.0093	0.45	231.6
b			
2739	0.050	1.21	131.2
2834	0.015	0.53	99.3
2855	0.062	0.25	11.2
2882	0.050	0.45	19.7

For the analysis of the experimental data we used the level scheme of Figure 6, where the two fundamentals are considered explicitly. Relaxation out of these two modes with  $\gamma_{07}$  and  $\gamma_{01}$  is assumed to be an irreversible process. This is justified if a potential back transfer (which should have a rate in the order of  $\gamma_{07}$  and  $\gamma_{01}$ ) from the accepting modes (overtones and combinations) is much slower than their decay rates  $\gamma_j$ . If we take the spectral widths  $\Delta\nu_j$  or the dephasing times  $T_{2j}$  of the accepting modes as a measure of their decay rates  $\gamma_j \leq 2\pi\Delta\nu_j$ , the analysis yields a consistent picture with  $\gamma_j \gg \gamma_{07}$  and  $\gamma_{01}$ . For the ratio of the internal rates connecting asymmetric and symmetric CH-stretching modes we assume that the principle of detailed balance holds:  $\gamma_{71} = \gamma_{17}g_7 \exp(-\Delta E_{17}/k_B T)$ . Where  $g_7$  is the degeneracy of state  $\nu_7$  and  $\Delta E_{17}$  is the energy difference  $\Delta E_{17} = E_7 - E_1$ .

For both molecules the experimental data (amplitudes related with the various rates and the rates themselves) can be used to invert the rate equation system and determine the microscopic rates of the reaction model (see Table 1). In both molecules the fastest relaxation out of the CH-stretching modes occurs from the symmetric  $\nu_1$  vibration. This relaxation channel has a time constant  $1/\gamma_{01} = 3.5$  ps and  $1/\gamma_{01} = 5$  ps for  $\text{CH}_2\text{CCl}_2$  and  $\text{CH}_3\text{CCl}_3$ , respectively. This observation is supported by the qualitative model of Fischer et al.,<sup>16,22</sup> where the vibrational energy relaxation should proceed via anharmonic coupling to overtones and combination bands of appropriate symmetry. We focus our discussion here on the relaxation out of the symmetric CH-stretching modes, where we can deduce the anharmonic coupling from the Raman intensities of the accepting modes of the same symmetry (see Figures 1a and 2a).<sup>23</sup> In Table 2 we present the time constants for the different relaxation channels calculated by using the formula given in ref 16.

$$\Gamma_{j1} = \frac{R_j}{(1 + R_j)^2} \exp\left[-\left(\frac{\omega_j - \omega_1}{\Omega}\right)^{2/3}\right] \frac{1}{T_{2j}} \quad (1)$$

with the frequencies  $\omega_j$  and the dephasing times  $T_{2j}$ .  $R_j$  describes the anharmonic coupling deduced from the Raman intensities  $I_j$  of the modes:  $R_j = I_j/I_1$ .  $\Omega$  is related to the interaction length

and the effective collision mass.<sup>16</sup> For small molecules and small energy transfer,  $\hbar|\omega_j - \omega_1| \leq k_B T$ ,  $\Omega$  is close to  $100 \text{ cm}^{-1}$ .<sup>16</sup> The intensities, frequencies, and dephasing times are deduced from the spontaneous Raman spectra of Figures 1a and 2a by a fit using Lorentzian functions. The total relaxation rate out of the  $\nu_1$  modes is obtained by summing over all relaxation channels  $\gamma_{01} = \sum_j \Gamma_{j1}$ . For  $\text{CH}_2\text{CCl}_2$  and  $\text{CH}_3\text{CCl}_3$  we obtain values of 3.4 and 6.3 ps, close to the experimental values of 3.5 and 5 ps, respectively (see Table 1). Considering the qualitative nature of eq 1 and uncertainties of finding all relaxation channels, this is a surprisingly good agreement.

In  $\text{CH}_3\text{CCl}_3$  the energy transfer between the CH-stretching modes, i.e., from the symmetric to the 2-fold degenerate asymmetric CH-stretching mode, takes  $1/\gamma_{71} = 4.7$  ps. This is equivalent with a rate  $\gamma = (9.4 \text{ ps})^{-1}$  for each individual relaxation channel. For  $\text{CH}_2\text{CCl}_2$  (where the accepting mode is nondegenerate) one finds  $1/\gamma_{71} = 9.5$  ps. It is interesting to note that this energy relaxation between two neighboring modes, where the same atoms are involved with very similar motions, is of the same order as or even slower than the relaxation out of the symmetric CH-stretching mode to overtones of completely different nuclear motion. In a simplified picture one may argue that the exchange between the two CH-stretching modes should be related to the dephasing time  $T_2$ . Since the difference in nuclear motion between asymmetric and symmetric CH-stretching modes is mostly a phase difference of the motion of one H-atom by  $180^\circ$ , single dephasing collisions could induce such a phase jump and with that the relaxation from one CH-stretching mode to the other. Thus the energy exchange should occur on the time scale of the dephasing process. From the spectral width of the Raman spectra the dephasing times  $T_2 = 1/(\pi\Delta\nu)$  can be deduced. Since  $T_2$  is conventionally defined to describe the decay of the vibrational amplitude, it has to be divided by two in order to account for intensity or population decays.<sup>21</sup> The relevant values are  $T_2/2 = 0.8$  ps and  $T_2/2 = 1.1$  ps for the symmetric CH-stretching modes of  $\text{CH}_2\text{CCl}_2$  and  $\text{CH}_3\text{CCl}_3$ , respectively. The considerably longer duration of the transfer time  $1/\gamma_{71}$  suggests that if the above-mentioned collision model applies, only very few of all phase-disturbing collisions are able to change the nuclear motion in such a way that a CH-stretching motion is converted to an antisymmetric one.

In conclusion, we have presented experimental results on fast vibrational relaxation between and out of different CH-stretching modes in liquids. We have shown that the excitation exchange occurs on the 5–10 ps time scale. In 1,1-dichloroethylene and 1,1,1-trichloroethane the dominant relaxation channel out of the CH-stretching modes is via the symmetric vibration. Here

several efficient reaction channels exist to close-lying overtone and combination bands of the same symmetry. For the asymmetric CH stretching mode where no accepting modes of appropriate symmetry were seen in the Raman spectra the relaxation is much slower. As a consequence the symmetry of the involved modes seems to be of dominant importance for the energy transfer process.

**Acknowledgment.** We thank S. F. Fischer for a number of helpful discussions on the theoretical background of ultrafast vibrational processes. This work was supported by the Deutsche Forschungsgemeinschaft.

## References and Notes

- (1) *Femtosecond Chemistry*; Wöste, J. M. a. L., Ed.; VCH Verlagsgesellschaft: Weinheim, 1995.
- (2) *Advances in Chemical Physics. Chemical Reactions and Their Control on the Femtosecond Time Scale XXth Solvay Conference in Chemistry*; Burghardt, P. G. a. I., Ed.; John Wiley: New York, 1997.
- (3) Klessinger, M.; Michl, J. *Excited States and Photochemistry of Organic Molecules*; VCH Publishers: New York, 1995.
- (4) Wolfseder, B.; Seidner, L.; Domcke, W.; Stock, G.; Seel, M.; Engleitner, S.; Zinth, W. *Chem. Phys.* **1998**, *232*, 323–334.
- (5) Wynne, K.; Hochstrasser, R. M. *Adv. Chem. Phys.* **1999**, *107*, 263–309.
- (6) Laubereau, A.; Linde, D. v. d.; Kaiser, W. *Phys. Rev. Lett.* **1972**, *28*, 1162–1165.
- (7) Deák, J. C.; Iwaki, L. K.; Dlott, D. D. *Chem. Phys. Lett.* **1998**, *293*, 405–411.
- (8) Seilmeier, A.; Kaiser, W. *Ultrashort Intramolecular and Intermolecular Vibrational Energy Transfer of Polyatomic Molecules in Liquids. In Ultrashort light pulses and Applications*; Kaiser, W., Ed.; Springer-Verlag: Heidelberg, 1988; pp 279–317.
- (9) Graener, H.; Zürl, R. *J. Phys. Chem. B* **1997**, *101*, 1745–1749.
- (10) Iwaki, L. K.; Deák, J. C.; Stuart, T. R.; Dlott, D. D. *Chem. Phys. Lett.* **1999**, *303*, 176–182.
- (11) Kolmeder, C.; Zinth, W.; Kaiser, W. *Chem. Phys. Lett.* **1982**, *91*, 323–328.
- (12) Hartl, I.; Zinth, W. *Opt. Commun.* **1999**, *160*, 184–190.
- (13) Band, Y. B.; Bavli, R. *Phys. Rev. A* **1987**, *36*, 3203–3217.
- (14) Hofmann, M.; Zürl, R.; Graener, H. *J. Chem. Phys.* **1996**, *105*, 6141–6146.
- (15) Iwata, K.; Weaver, W. L.; Gustafson, T. L. *Chem. Phys. Lett.* **1993**, *210*, 50–54.
- (16) Fendt, A.; Fischer, S. F.; Kaiser, W. *Chem. Phys.* **1981**, *57*, 55–64.
- (17) Winter, F.; Hummel, D. O. *Spectrochim. Acta* **1966**, *23A*, 1839–1861.
- (18) Yamaoka, Y.; Machida, K. *J. Mol. Spectrosc.* **1980**, *83*, 21–30.
- (19) Allen, G.; Bernstein, H. J. *Can. J. Chem.* **1954**, *32*, 1124–1141.
- (20) Frankiss, S. G.; Harrison, D. J. *Spectrochim. Acta* **1975**, *31A*, 29–39.
- (21) Laubereau, A.; Kaiser, W. *Rev. Mod. Phys.* **1978**, *50*, 607–665.
- (22) Fischer, S. F.; Laubereau, A. *Chem. Phys. Lett.* **1978**, *55*, 189–196.
- (23) McKean, D. C. *Spectrochim. Acta* **1973**, *29A*, 1559–1574.